DOI: 10.1002/cbic.200800324

Theoretical Study of the Human Bradykinin–Bradykinin B2 Receptor Complex

Artur Gieldon,[a] Jakob J. Lopez,[b] Clemens Glaubitz,[b] and Harald Schwalbe*[a]

The interaction of bradykinin (BK) with the bradykinin B2 receptor (B2R) was analyzed by using molecular modeling (MM) and molecular dynamics (MD) simulations. A homology model for B2R has been generated and the recently determined receptor-bound solid-state NMR spectroscopic structure of BK (Lopez et al., Angew. Chem. ***2008****,* 120*, 1692–1695;* Angew. Chem. Int. Ed. ***2008****,* 47*, 1668–1671) has been modeled into the binding pocket of the receptor to probe the putative ligand–receptor interface. The experimental hormone structure fitted well into the binding pocket of the receptor model and remained stable during the MD simulation. We propose a parallel orientation of the side chains for Arg1 and Arg9 in BK that is bound to B2R. The MD simulation study also allows the conformational changes that lead to the activated form of B2R to be analyzed. The hydrogen bond between N140 (3.35) and W283 (6.48) is the key interaction that keeps the receptor in its inactive form. This hydrogen bond is broken during the MD simulation due to rotation of transmembrane helix 3 (TM3) and is replaced by a new hydrogen bond between W283 (6.48) and N324 (7.45). We propose that this interaction is specific for the activated form of the bradykinin B2 receptor. Additionally, we compared and discussed our putative model in the context of the structural model of the partially activated rhodopsin (Rh*) and with the known biochemical and structural data.*

Introduction

Bradykinin (BK) (Arg-Pro-Pro-Gly-Phe-Ser-Pro-Phe-Arg) is a nonapeptide autacoid generated from plasma globulins and synthesized in the liver.[1,2] A large variety of biological effects have been reported for bradykinin. Most of them are mediated by two G protein-coupled receptors (GPCRs) B1R and B2R[3,4,5] and transduced through interaction with the heterotrimeric G proteins.[6] Vasodilatation and control of vascular tone,[7] ion transfer in epithelia,[8] the prostaglandin–NO cascade,[9] and pain[10] are mediated by B2R.[2,11] If B2R is inactivated, those functions can be induced by upregulation of B1R.[12,13] BK induces cell proliferation,[14] proliferation of the breast epithelium,[15] and proliferation of breast cancer.[16] Bradykinin receptors can be a target for developing a chronic epilepsy treatment.[17,18] Bradykinin also plays some role in higher brain functions[19] and has been proposed as a physiological milk ejection stimulant.[20]

Computational studies have previously been performed to investigate hormone/ligand–GPCR complex structures at the molecular level.[21,22] Two crystal GPCR structures have been solved: the ground state rhodopsin (Rh) structure[23,24] and the inactive form of the β_2-adrenergic receptor (β2ADR).[25,26] In addition, X-ray structural analyses have provided a model for partially activated rhodopsin (Rh*).[27]

It has been demonstrated that solid-state NMR spectroscopy can be used to derive the conformation of peptide ligands bound to GPCR receptors reconstituted in a membrane environment. Previously, we have reported a model derived from solid-state NMR spectroscopy of the backbone structure of the receptor-bound bradykinin, which represented the second NMR investigation of GPCR–ligand complexes[28] after the backbone structure of neurotensin bound to the neurotensin receptor was reported by Luca et al.[29]

Our previous solid-state NMR investigation of BK provided information on the backbone conformation only. Here, we use MD simulations to derive the side-chain conformation of the receptor-bound BK and to predict the initial conformational changes of the bradykinin-induced activation. Only one of four conceivable binding modes was able to induce conformational changes that were specific to, and in agreement with biochemical data on the activated form of bradykinin B2 receptor and on the proposed interaction with kallidin, a B1R agonist that is very similar to BK.[30] According to our simulations, the initial changes in the conformation of the bradykinin receptor involve a rotation of transmembrane helix 3 (TM3) accompanied by a change of hydrogen bond interactions of W283 (6.48) with N140 (3.35) in the apo form to a hydrogen bond with N324 (7.45) in the holo form of the receptor.

[a] *Dr. A. Gieldon, Prof. Dr. H. Schwalbe*
Johann Wolfgang Goethe-Universität
Institute for Organic Chemistry and Chemical Biology
Center for Biomolecular Magnetic Resonance (CBMR)
Max-von-Laue-Strasse 7, 60438 Frankfurt (Germany)
Fax: (+49) 69-7982-9515
E-mail: schwalbe@nmr.uni-frankfurt.de

[b] *Dr. J. J. Lopez, Prof. Dr. C. Glaubitz*
Johann Wolfgang Goethe-Universität, Institute for Biophysical Chemistry
Center for Biomolecular Magnetic Resonance (BMRZ)
Max-von-Laue-Strasse 7, 60438 Frankfurt (Germany)

Results and Discussion

The ligand–receptor interface

Simulation results: The backbone structure previously determined by solid-state NMR spectroscopy[28] combined with information on the available conformational space inside the receptor pocket revealed two possible models for the orientation of the arginine side chains. In both cases, they are found within one plane but with parallel ("C" like) or antiparallel ("Z" like) orientations (Figures 1 and 2). After the backbone imposition we observed that the planes that were defined by the arginine side chains in "Z"-like and "C"-like conformations are rotated by 80° relative to each other. Three different stable ligand–receptor complexes were built (see Figure 1). The receptor residues in the ligand vicinity can be classified as being either involved in direct ligand interactions or as sterically constituting the border of the binding pocket with only weak BK interactions. Residues found at the BK binding pocket border are I117 (2.64), L129 (EL1), V133 (3.28), I137 (3.32), L141 (3.36), L188 (4.56), T224 (5.38), L228 (5.42), T294 (EL3), Y322 (7.43). No border residue is found for TM1, and only a single residue is found for TM7. Residues L117 (2.64), I137 (3.32), L141 (3.36), L228 (5.42) are placed on the bottom of the pocket, whereas the remaining residues are placed on the "walls".

The residues that are involved in more direct BK–B2R interactions are summarized in Table 1. As a result of our ligand-docking calculation, the same B2R residues are found to interact with Arg1 in complexes B and D, and with Arg9 in complex A. After the MD simulation, only a single salt bridge between E51 and Arg1 (complex B, D) and Arg9 (complex A) remained as an interaction that was found in all three computed systems. An additional salt bridge between Arg1 and D311 (7.32), a hydrogen bond between Arg1 and Q315, and hydrophobic interactions between Pro2 and W123 (EL1) are found in complexes B and D only. The only interaction present in all three complexes A, B, and D is a close side-chain–side-chain contact between Phe5 and F286 (6.51). In complex D, Phe5 interacts only with the F286 (6.51) backbone. In this case, the side chain of Phe5 is directed towards L129 (EL1) which is placed on the other site of the pocket. The interactions that are present in complex D are given in Figure 3.

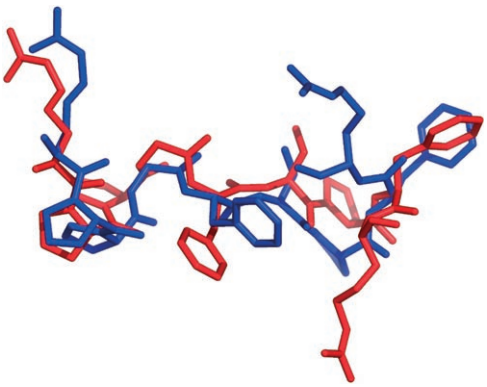

Figure 2. The BK solid-state NMR spectroscopic backbone structure together with predicted side-chain orientations reveals two possible models with "C" like (navy) and a "Z" like (red) conformation. In both cases, Arg1 and Arg9 are in plane with the membrane/receptor normal, but with parallel or antiparallel side-chain orientation.

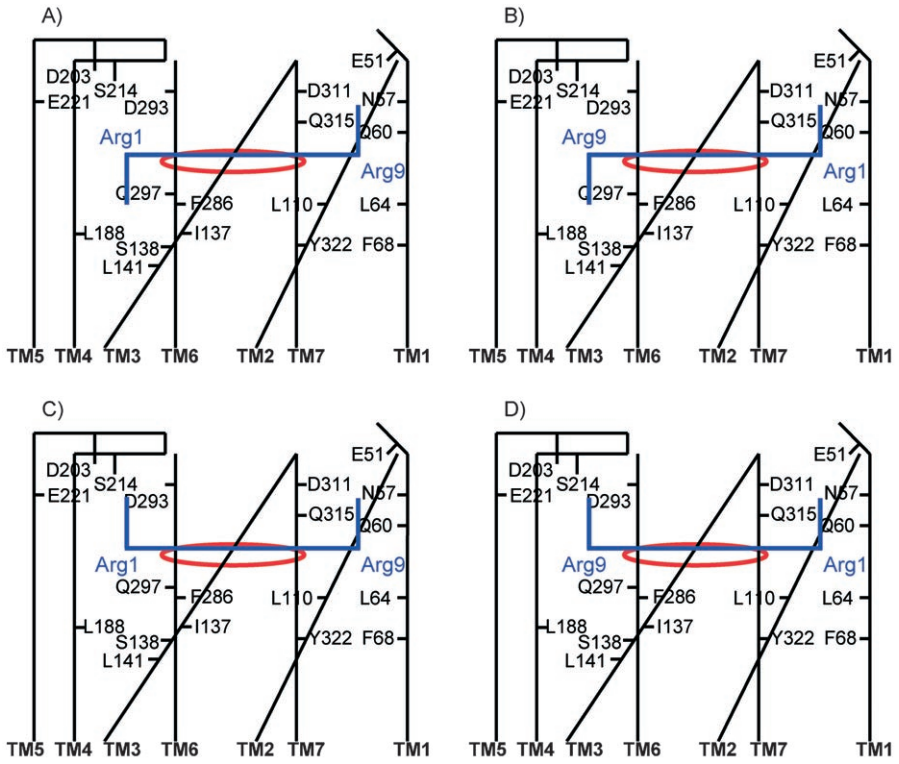

Figure 1. Schematic representation of the B2R receptor pocket with bound bradykinin. Conserved and essential B2R residues used for the docking procedure are labeled. The space occupied by retinal in rhodopsin is highlighted as an ellipse. A), B), C) and D) correspond to the four possible orientations of the ligand in the receptor binding pocket. The amino acids of bradykinin are represented by a blue line, and amino acid annotations for the N and C-terminal amino acids Arg1 and Arg9 are given by using the three-letter code.

Discussion

The binding pocket in the context of biochemical data

As summarized in Table 1, four out of 16 residues identified on the BK–B2R interface (S138 (3.33), M192 (4.40), F286 (6.51) and T290 (6.55)) and four out of ten residues identified on the border of the receptor binding pocket (I137 (3.32), L141 (3.36), L228 (5.42) and Y322 (7.43)) were shown to face the binding pocket in class A GPCRs.[49] The

Table 1. Summary of the residues found on the B2R–BK interface.

Residue in BR	Complex A	Complex B	Complex D
Arg1	N134 (3.29), S138 (3.33), M192 (4.40), S214 (EL2), E221 (EL2)	E51 (N-term), D311 (7.32), Q315 (7.36)	E51 (N-term), Q60 (1.35), D311 (7.32), Q315 (7.36)
Pro2	N225 (5.39)	W123 (EL1)	W123 (EL1)
Pro3	N225 (5.39), F286 (6.51), T290 (6.55)	W52 (N-term), S318 (7.39)	A114 (2.61)
Gly4	I213 (EL2)	I213 (EL2)	
Phe5	I213 (EL2), F286 (6.51)	I213 (EL2), F286 (6.51)	W123 (EL1), L129 (EL1), F286 (6.51)
Ser6	V133 (3.28)	S214 (EL2)	N134 (3.29), F286 (6.51), T290 (6.55)
Pro7	Q315 (7.36), S318 (7.39)	N225 (5.39), T290 (6.55)	N134 (3.29), S138 (3.33), F286 (6.51)
Phe8	Q60 (1.35), A114 (2.61), F319 (7.40)	N134 (3.29), E221 (EL2), N225 (5.39)	N134 (3.29), S138 (3.33), L228 (5.42)
Arg9	E51 (N-term), W123 (EL1)	N134 (3.29), S138 (3.33), M192 (4.60), S214 (EL2), F286 (6.51), T290 (6.55)	M192 (4.60), I213 (EL2), S214 (EL2), E221 (EL2)

mutagenesis data presented in ref. [37] indicate that some of the border residues identified in our MD simulation (I137 (3.32), L141 (3.36) and Y322 (4.43)) do not affect BK binding. The situation is different for residues identified during the MD simulation to be located at the receptor interface: only M192 (4.60)) has no effect on the BK binding affinity,[35] and three residues (D311 (7.32), Q315 (7.36) and Y322 (7.43)) were shown to have only a small effect. Four residues (S138 (3.33), F286 (6.51), T290 (6.55) and D311 (7.32)) were described in ref. [35] to be crucial for BK binding affinity. S138 (3.33) was postulated to be involved in the recognition of the binding specificity of peptidic ligands .[57]

We also compared our findings with the B1R–DALK (bradykinin B1 receptor-([Leu9]DesArg10 Kallidin) KRPPGFSPL–B1R antagonist) and B1R–DAK (DesArg10 Kallidin) KRPPGFSPF–B1R agonist) interface, that was obtained by homology modeling and mutagenesis studies.[30] Mutations of D291, F302 (D311, Y322 in positions 7.32 and 7.43 in B1R and B2R, respectively) cause a significant decrease in the affinity both for the antagonists and agonists. D311 (7.32) seems to be important because it interacts with Arg1 in complex B and D (this interaction was not observed in complex A). The third residue from TM7 in position 7.35–L294 (in B2R, T314) seems to have a stronger influence on the binding affinity of agonists than of antagonists, but we did not observe any interaction in our models. Ha et al.[30] also observed a hydrophobic interaction of the antagonist with I192 from EL2. We found a similar interaction of bradykinin with I213 at a position that differs by one place. The other similar identified interactions are I97, I117 (2.64); N114, N134 (3.29); A270, T290 (6.55); Y266, F286 (6.51); Q295, Q315 (7.36) in B1R, B2R, respectively.

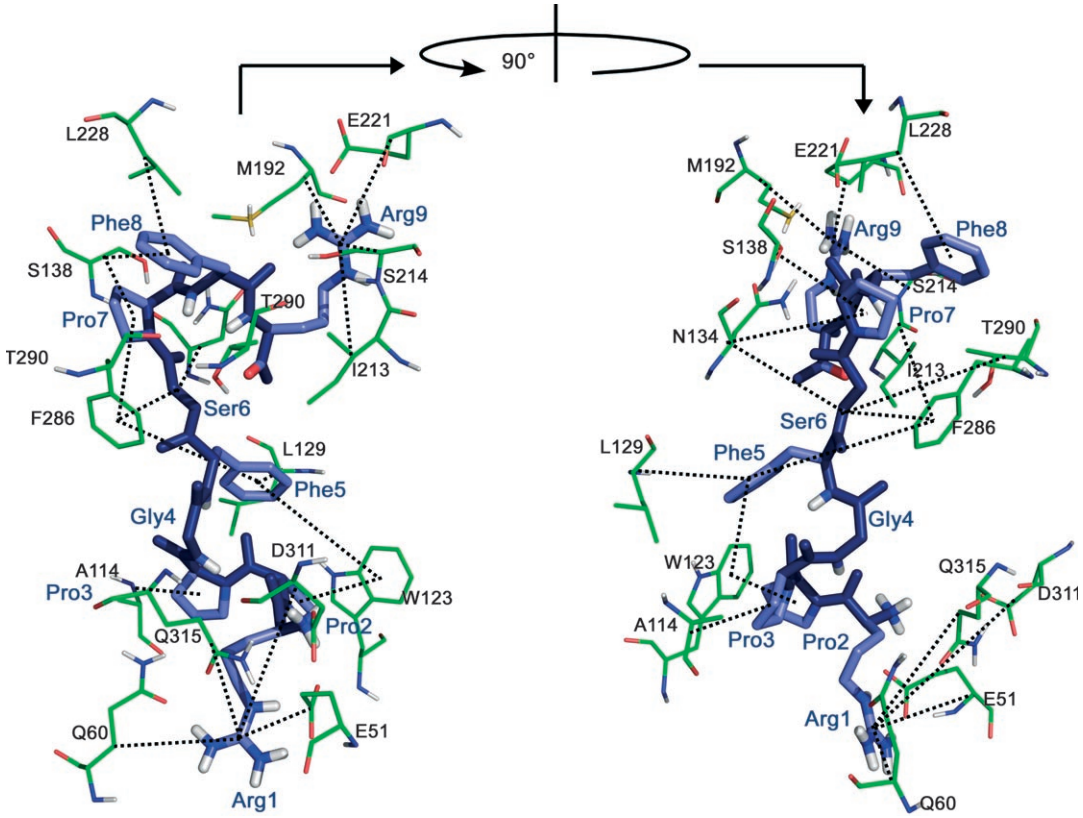

Figure 3. All interactions that were observed in complex D.

Activation of B2R by bradykinin

Simulation results and model selection: We have used the high-resolution crystal structure of rhodopsin (dark)[23,24] as a template for the modeling of the bradykinin receptor (B2R) and for docking bradykinin (BK). This model corresponds to the inactive state of B2R, but we assume that during the MD simulation, conformational changes in B2R are induced by the binding of BK that are specific for the activated form of the receptor. We are aware of the fact that 2 ns simulation time is not sufficient to fully activate the receptor because milliseconds are required for the full activation trajectories.[58] Nevertheless, the observed conformational changes can provide some information about the initial stage of the activation process.[59] Our findings can be discussed in the context of a model for the partially activated rhodopsin (Rh*; PDB ID: 2i37),[27] and based on experimental data.[27,60,61,62] The sequence homology between Rh and B2R and between B2R and β2ADR is similar; there are approximately 65 identical and 35 similar residues in both cases. The homology between RH and β2ADR is less, with 50 identical and 25 similar residues. Therefore, some similarities with the structure of β2ADR should be observed as well.

After the MD simulation, only small structural changes with an RMSD (calculated from the starting model and the last snapshot of the simulation for all C_α atoms) of 3.5; 3.3; 2.8 Å for the BK–B2R complexes A, B, and D were observed. For a detailed comparison of these three models with that of the partially activated rhodopsin (Rh*), three planes at the top, in the middle and at the bottom of the receptor were defined. We have assigned one residue from each helix to each plane.[33] By measuring the distances between all Cα atoms of these residues within one plane, we were able to determine, which of the three computed models (complexes A, B, and D) is the most similar to the model of the partially activated rhodopsin (Rh*). This comparison also allows us to find the most likely features of the active bradykinin receptor state.

In all three models, the extracellular side of TM2 moved slightly away from the receptor core. For example, the distances between C_α atoms of residues 2.64 and 4.61 are found at 18.9; 21.5; 18.1; 22.1; 21.3; 20.8 Å, and between residues 2.64 and 7.32 at 15.1; 21.8; 19.2; 17.3; 15.2; 14.1 Å in the B2R starting model, in the BK–B2R complexes A, B, D, in the partially activated rhodopsin model and in the β_2-adrenergic receptor structure, respectively.

Notably, we observe a significant conformational change for the position of the intracellular part of TM7. In all calculations, this part moved away from the receptor core. The distance changes during the MD simulation are small when compared with the activated form of rhodopsin and large compared to the inactivated form of β2ADR, and are given as follows: 2.39–7.53 by 0.8 and 4.3 Å; 3.50–7.53 by 0.4 and 3.5 Å and between 4.42–7.53 by 0.9 and 3.3 Å in Rh* and β2 ADR, respectively. We note that the distances in all the computed systems differ by no more than 1 Å from the β2ADR structure; this makes them more similar to β2ADR than to the structure of light-activated Rh*.

Furthermore, we have performed a detailed analysis of the rotation of every TM helix in the receptor core as described in ref. [63]. Models before and after the MD simulation were superimposed (all rotations are described as viewed from the extracellular side of the receptor). In complex D, TM3 rotates 10° counterclockwise during the simulation. This rotation of TM3 relative to the starting structure, in which the ligand had been placed into the binding pocket, makes complex D the best-fitting model to the Rh* model. With a relatively high rotation energy profile of TM3[58] it is unlikely that this rotation is coincidental. We did not observe any TM3 rotation in the other computed systems. Additionally, TM4 in the complex D exerts a small clockwise rotation. The same degree of TM4 rotation can be observed in 2RH1 β_2-adrenergic receptor in comparison to the dark-state structure of rhodopsin.

The observation that the hydrogen bond between N(3.35) and W(6.48) was broken only in complex D provides the most important evidence to support the MD simulation result of complex D as the most probable form of the B2R activated state. This hydrogen bond was reported in refs. [35–37] to be essential to maintain the inactive form of the receptor. To analyze the conformational changes during the simulation in more detail, we analyzed the dynamics of the hydrogen bonding switch throughout the MD trajectory (Figure 4).

In the starting structure, the distances between N_ε of W283 (6.48) and O_δ of N140 (3.35) and between N_ε of W283 (6.48) and O_δ of N324 (7.45) are both found at 3.1 Å. The N_ε from W283 (6.48), however, is directed towards N140. In complex A and B, high fluctuations of this distance between 3 and 7 Å can be observed during the entire simulation. In complex D, the distance is stabilized at ~6 Å after 1.4 ns. This is caused by the rotation of TM3. In complexes A and B, this rotation is not observed and any deviations we can observe are caused by the conformational flexibility of the N140 (3.35) and W283 (6.48) side chains. After the rotation of TM3, N324 (7.45) is the only partner in the vicinity of W283 (6.48) to build a hydrogen bond, which in fact remained stable after 1.9 ns with a deviation no more than 1 Å. In the complex A and B, the N_ε W283 (6.48)-O_δ N324 distance is maintained at ~4 Å. (Figure 5)

The MD simulations are in good agreement with a commonly accepted hypothesis that GPCRs exist in two forms in the cellular membrane and that the binding of the ligand shifts this conformational equilibrium to one form or another.[31] In complex D, we can observe a very large increase of the N_ε W283 (6.48)–O_δ of N140 (3.35) distance up to 7.8 Å at the beginning of the simulation. After 1.9 ns, this distance is stabilized at the range of ~6 Å, while in conformations A and B, the N_ε W283 (6.48)–O_δ of N140 (3.35) distance changes from ~3 to ~6 Å. We conclude that complexes A and B represent "wrong" models for which receptor activation cannot be observed.

Complex D of the BK/B2R complex corresponds to the activated state of B2R

In rhodopsin, the transmembrane region is stabilized by a number of interhelical hydrogen bonds and hydrophobic interactions.[23,24] During the activation process of rhodopsin, modu-

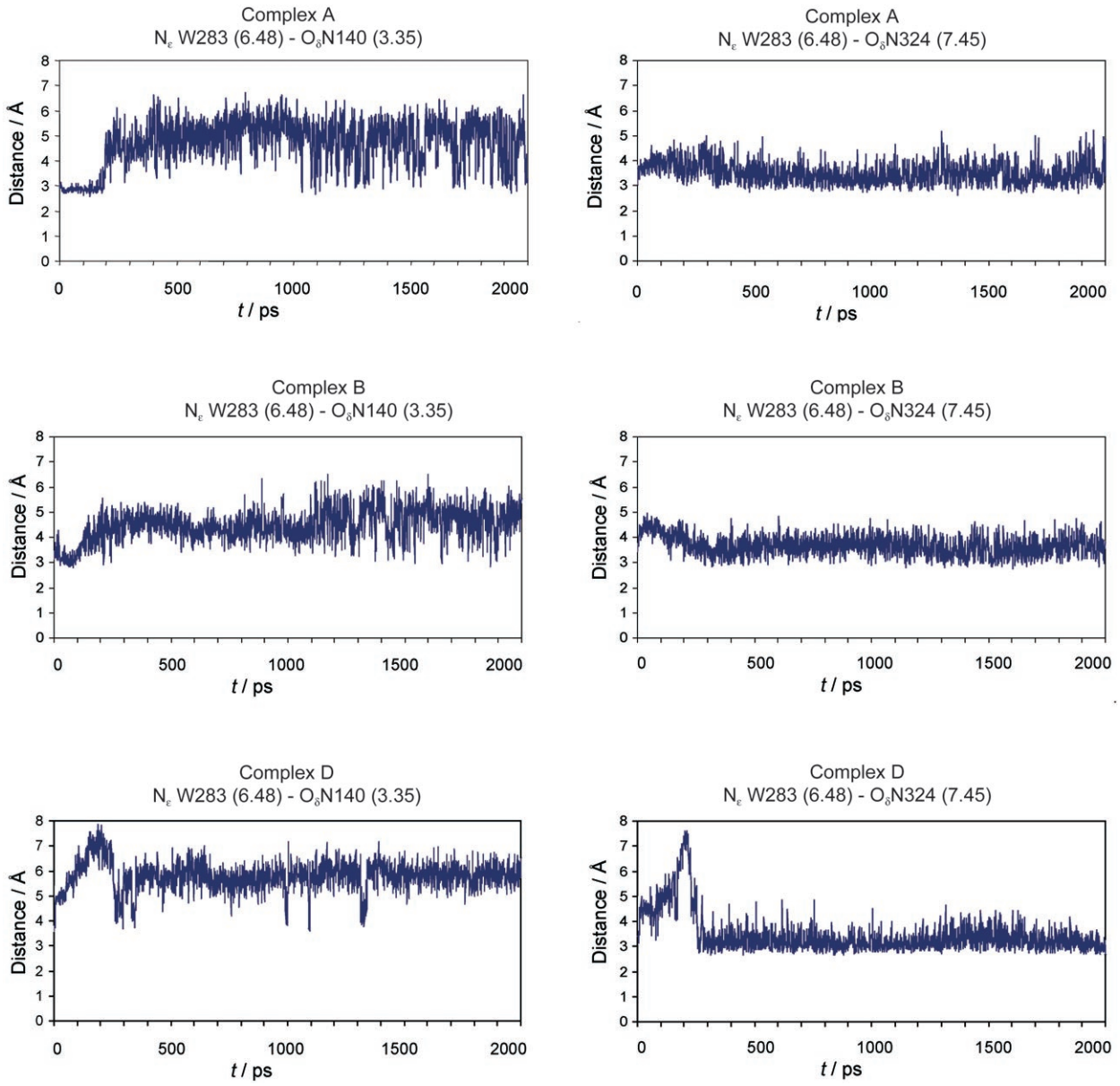

Figure 4. Distance plots of the residues essential for the switching process between inactive and activated form of the B2R. The interatomic distance was measured in the snapshots that were taken every 1 ps. The hydrogen bond between W283 and N140 is essential to maintain the inactive form of B2R. In complex D, this bond is broken and new bond between W283 and N324 is formed, whiles for complexes A and B, this bond is not broken permanently.

lations of the interaction network are observed for TM5–TM7, while TM1–TM4 form a core that remains very stable.[64]

Our simulation indicated that in the bradykinin receptor, the interface between TM2 and TM3 is located around Y95 (2.42) for TM2, and Y142 (3.37) and F147 (3.42) for TM3 forming three interaction clusters (Figure 6, Table 2).

1) Y95 (2.42) interacts with L150 (3.45), V151 (3.46) and forms a hydrogen bond with D154 (3.49) from the (E/DRY) motif.
2) Y142 (3.37) interacts with T185 (4.53) and L188 (4.56).
3) F147 (3.42) interacts with L96 (2.43) and L99 (2.46); this triggers the interaction of L96 (2.43) with F82 (1.57).

Additionally, we found several stable interactions within the TM1–TM4 core: P61 (1.36)–I115 (2.62), F68 (1.43)–P111 (2.58), I76 (1.51)–L104 (2.51), I94 (2.41)–A174 (4.42), I105 (2.52)–I136 (3.31), W113 (2.60)–V132 (3.27), L150 (3.45)–Y177 (4.45). Noteworthy is the stable interaction between N75 (1.50)–D103 (2.50)–N140 (3.35) that has been reported to play a role in the receptor activation process.[22]

TM4 is placed outside the receptor core; this results in a smaller number of interactions.[63] Nikiforovich and Marshall[58] showed for rhodopsin that the energy profile of the rotation of TM4 is low and flat. This observation is considered to be true for the entire class A family and implies that the interactions between TM4 and the rest of the helices are weak.

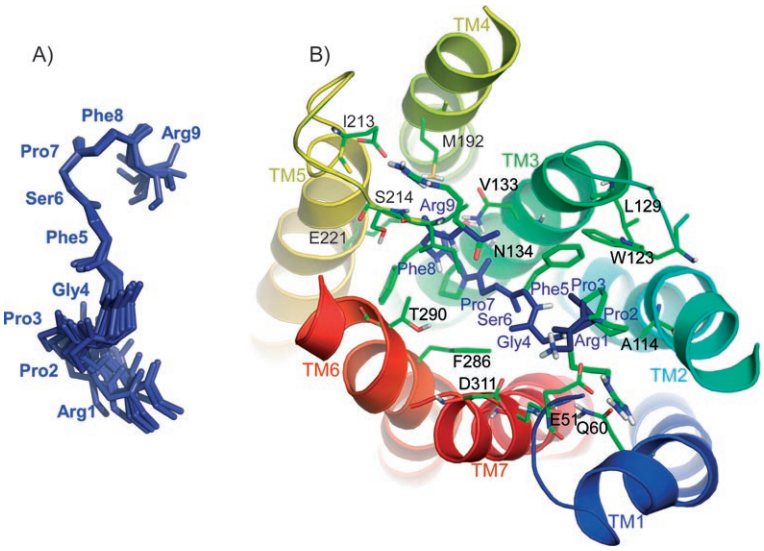

Figure 5. A) The structural ensemble that was derived from solid-state NMR spectroscopic experiments. B) Graphical representation of the activated B2R model. The helices are colored as follows: TM1: blue, TM2: cyan, TM3: green, TM4: lime green, TM5: yellow, TM6: orange, TM7: red. The ligand backbone is dark blue.

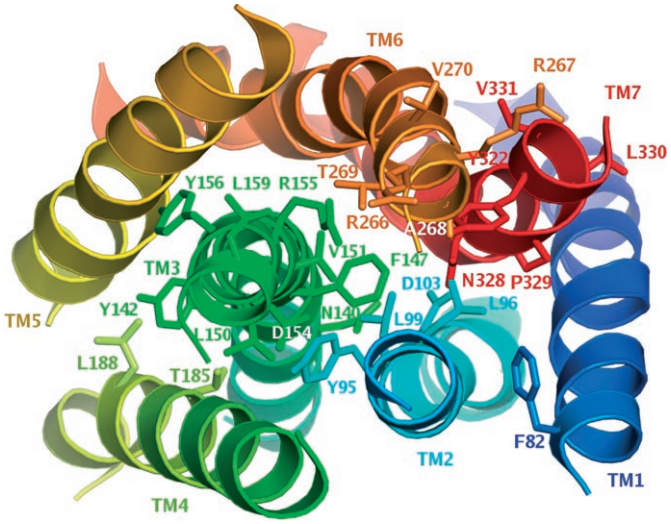

Figure 6. The view from the extracellular side of the activated form of B2R. The most relevant interactions with the highly conserved motifs DRY (154–156) from TM3 and NPLVY (328–332) from TM7 and the most relevant residues in the vicinity are presented. The helices were colored as follows: TM1: blue, TM2: cyan, TM3: green, TM4: lime green, TM5: yellow, TM6: orange, TM7: red.

Conformational changes in rhodopsin have been experimentally determined by EPR distance measurements,[63] which indicated that during the activation, the intracellular parts of TM3 and TM6 move closer to each other. This movement is very important, because it is responsible for conformational change of the E/DRY motif (B2R–DRY 154–156), which is significant for G protein coupling.[65,66]

We identified a hydrogen bond between D154 (3.49) and Y95 (2.42), which remains stable during the simulation. In addition, the neighboring residue R155 (3.50) is hydrogen bonded with T269 (6.34) (this corresponds to the hydrogen bond with T251 in rhodopsin), and participates in a salt bridge with E265 (IL3), which becomes weaker as a consequence of the drift of the third intracellular loop. The hydrogen bond between the next amino acid Y156 (3.51) and Q246 (5.60) that are present in the dark-state rhodopsin structure is broken at the end of the simulation.

The data that were presented by Nikiforovich and Marshall[58] show that during the activation process of rhodopsin, the cytoplasmic parts of TM1 and TM7 move away from each other by 2–4 Å. These results are additionally supported by EPR measurements[63] on rhodopsin that suggested that the distance between residues in positions 1.56–7.50 should increase by 2.5 Å. In Rh*, it was increased by 1.1 Å, and in the β2-ADR it decreased by 0.5 Å in comparison to inactive rhodopsin. In our model, the distance between residues in positions 1.56–7.50 was increased by 0.2 Å. This observation supports the view that both Rh* and our MD model show the initial events of the activation process.

Table 2. Summary of the residues involved in the B2R activation with homologous rhodopsin residues.

Rhodopsin	B2 bradykinin receptor	Universal residue number[33]	Refs.
N55	N75	1.50	[22,67]
D83	D103	2.50	[35,49]
G120	N140	3.35	[35,36]
C264	C282	6.47	[69]
W265	W283	6.48	[35,37,49,69]
Y268	F286	6.51	[35]
K296-RET	Y322	7.43	[35,37]
S298	N324	7.45	this paper
N302	N328	7.49	[22,67]

Next, we discuss the conformational changes for TM7 that are highly relevant, because the most conserved motif (NPXXY, B2R–NPLVY (328–332)) that is responsible for receptor activation is located in TM7[67] and Y332 (7.53) seems to be the most important residue from the NPLVY motif, due to direct involvement in signal transduction.

In our starting model, Y332 (7.53) interacts with F82 (1.57) and L96 (2.43) and is hydrogen bonded to E93 (IL1), which corresponds to residue N73 (IL1) in rhodopsin. After the simulation, this hydrogen bond and the hydrophobic interaction with F82 (1.57) are lost, and the side chain is placed between L96 (2.43) and L271 (6.36). Amino acids L330 (7.51) and V331 (7.52) are turned outside toward the membrane and P329 (7.50) probably supports the bending of TM7 into a proper position. N328 (7.49) forms a hydrogen bond with D103 (2.50) (Figure 6). During the activation process, contacts between intracellular parts of TM2 and TM7 are broken[68] in agreement with our findings. The NPLVY motif is interacts with the interface of TM1 and TM2 and D103 (2.50) is placed in the center of

a large hydrogen-bond network. In our model, D103 (2.50) is involved in hydrogen bonds with: N75 (1.50), N140 (3.35), N324 (7.45) and N328 (7.49) from the NPXXY motif.

The hydrogen bond between N140 (3.35) and W283 (6.48) (see Computational Methods and Figure 7)[35] plays the key role in the maintenance of the inactive form of the B2 receptor. As a consequence of the TM3 rotation, the initial hydrogen bond can no longer be formed and is replaced by a hydrogen bond between W283 (6.48) and N324 (7.45) (see Figure 7). We postulate that this hydrogen bond is formed as the replacement for the N140 (3.35)–W283 (6.48) H-bond and plays an important role in the maintenance of an activated form of the bradykinin B2 receptor. W283 (6.48) remained in the 1HZX rhodopsin-like conformation,[23,24,35,69] with the indole ring directed to the extracellular side of the receptor. The conformational change of W283 (6.48) was postulated by Shi et al.[69] for the β_2-adrenergic receptor activation, during which the distance between C (6.47) and W283 (6.48) is proposed to increase. In our model, we observed small changes as well. The distances between the C_β atom of cysteine (C282 (6.47)) and the $C_{\delta 1}$ atom of tryptophan (W283 (6.48)) increase from 3.96 to 4.49 Å during the simulation. The conformational change described by Shi et al.[69] is not possible for B2R because of the steric clash caused by L141 (3.36). The corresponding valine residue (V117) in the β_2-adrenergic receptor is small enough to allow for a conformational change. As a consequence, the differences in position 3.36 between B2R and β2ADR might modulate the receptor activation mechanism.

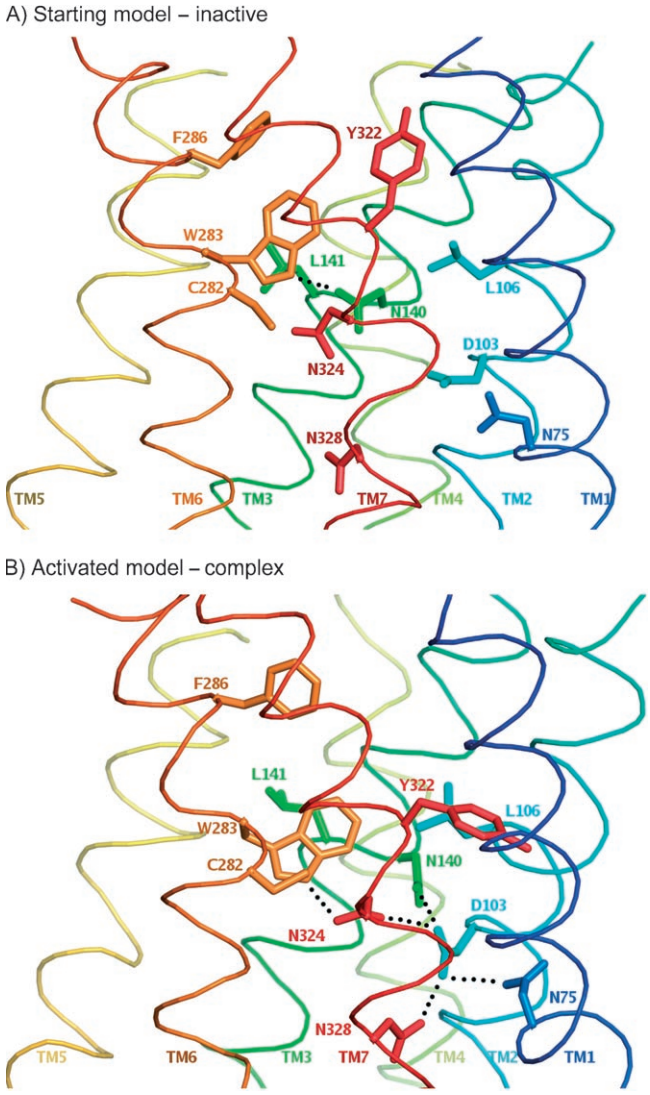

Figure 7. Inactive (left) and activated (right) B2R model. The residues that are involved in the receptor activation are summarized in Table 3. The receptor is in the rope representation: TM1: blue, TM2: cyan, TM3: green, TM4: lime green, TM5: yellow, TM6: orange, TM7: red.

F286 (6.51) is another residue that is potentially relevant for the activation process and is found one helix turn away from W283 (6.48). According to ref. [35] the interaction of W283 (6.48) with F286 (6.51) is present in the intermediate/active state of B2R, based on modeling and biochemical data. We found that F286 (6.51) is crucial for ligand binding (Figure 3), but according to our model the interaction with W283 (6.48) is very weak (the distance between closest side-chain atoms is more than 5 Å). The other postulated interactions of F286 (6.51) are with residues (N140 (3.35)–D103 (2.50)–Y322 (7.43)).

We observed, however, a hydrogen bond between N140 (3.35) and highly conserved D103 (2.50) only. In the starting structure, this bond is quite weak and after the simulation the N140 (3.35)–W283 (6.48) hydrogen bond is lost and N140 (3.35) changes its conformation in the receptor pocket by turning towards hydrogen bond network with D103 (2.50) in the center. As a consequence the D103 (2.50)–N140 (3.35) hydrogen bond distance decreases (Figure 7).

In the dark-state rhodopsin-like models, Y322 (7.43) cannot create a hydrogen bond with D103 (2.50) and N140 (3.35) as postulated in ref. [35] According to the computer mutation of the rhodopsin structure, the Y322 (7.43) side chain occupies the place of the original K296 (connected by the Schiff's base formation with retinal molecule) and is directed towards the extracellular side of the receptor. After the simulation, the Y322 (7.43) side chain becomes directed towards TM1 and TM2, most probably because of the Pro3 of the bradykinin hormone. However, it is not possible to change it "down" because this place is already occupied by L106 (2.53). Therefore the hydrogen-bond network between residues (N140-D103-Y322) that are postulated in ref. [35] in the dark-state rhodopsin-like model is not possible.

The conformation of bound Bradykinin (BK)

Our ligand-docking procedure revealed that the experimentally determined receptor-bound backbone structure of BK can only be placed in the binding pocket when the side chains for Arg1 and Arg9 are in plane and parallel or antiparallel (Figure 1 "Z"-like and "C-"like). Four possible models for the ligand–receptor complex have been suggested (Figure 1) but we restrict our discussion to the "C"-like complex D because only for D have hints towards receptor activation upon BK binding been obtained.

During the MD simulation, the backbone structure remained basically the same, but the side-chain conformations adapted

to the receptor interface. The largest side-chain variation is observed for the χ_1 torsion angle of Phe5 (Table 3).

Phe5 interacts with F286 (6.51), which plays an important role in the receptor activation and is involved in direct interaction with the ligand.[35] L129 (EL1) significantly influences the conformation of Phe5 (see Figure 3). As a result of the docking procedure, we found a χ_1 angle of -147° in model D for Phe5. After the MD simulation this angle changed significantly to -58°. Our data also show that only the "C"-like conformation with parallel and planar Arg1 and Arg9 side chains was able to induce the changes in the B2R model that are specific to the activated form of the receptor.

Earlier simulation studies (Kyle et al.)[70] or a receptor mimic[71] and experiments in the micelle[72] agree with the overall twisted S-shape of the bound ligand backbone, but disagree in many details, which is presumably due to the smaller number of experimental restraints.

Conclusions

The aim of the present study was to characterize and identify the bradykinin (BK) conformation and bradykinin receptor (B2R) binding interface by using molecular dynamics (MD) simulation in an explicit solvent, in combination with solid-state NMR spectroscopic results. The crystal structure of dark-state rhodopsin[23,24] (1HZX) was used as a template for the bradykinin B2 receptor model building. To date, this experimental structure is the most widely used choice to model a receptor of the class A GPCR family.[21,49] We successfully identified the bradykinin (BK) conformation that was bound to the receptor. The conformation remained stable during the simulation.

We could indicate changes specific for the initial steps in the activation process. The extracellular part of TM2 and the intracellular part of TM7 moved away from the receptor core. The most significant conformational change, however, is connected with the rotation of TM3. The hydrogen bond between N140 (3.35) and W283 (6.48) plays the key role in the maintenance of the inactive form of the B2 receptor. As a consequence of the TM3 rotation, this bond is broken and replaced by a hydrogen bond between W283 (6.48) and N324 (7.45). From our simulations, we propose that the hydrogen bond is formed as a replacement for the N140 (3.35)–W283 (6.48) H-bond and plays a role in the maintenance of the activated form of the bradykinin B2 receptor.

We identified a set of residues that are responsible for the ligand–receptor interaction. F286 (6.51) is involved in the receptor-activation process, but mostly it interacts with the ligand. We identified this interaction in all our models. It is responsible for the conformational change of the Phe5 χ_1 torsion angle. The experimentally obtained backbone structure during the simulation remained intact. The highly conserved motifs such as E/DRY and NPXXY at the receptor–G protein binding interface allow the class A GPCR family to share a common activation mechanism,[31,73] the detailed rearrangement at atomic level will, however, show some differences between different members of the class A GPCR family. For example during the activation of the β_2-adrenergic receptor, W (6.48) increases the distance between C (6.47) by turning towards the receptor core.[69]

The study shows that the experimentally determined conformation of the complex by solid-state NMR spectroscopy helps to drive molecular modeling and molecular dynamics studies of GPCR–ligand complex structures. The identified interactions are important for future studies: Due to the abundance of the bradykinin–bradykinin receptors system, the study of the BK–BR complex that is supported by our recent solid-state NMR spectroscopic investigation might guide the rational design of new potent ligands.[74,75]

Computational Methods

BK structure determination: The BK backbone structure was obtained from experimental restraints that were derived from solid-state NMR experiments as previously described. The structural models for the ligand converged to an average backbone RMSD of 0.49 ± 0.16 Å.[28]

Building a B2R model: Bradykinin receptors B1 and B2 belong to the class A family of the rhodopsin-like GPCRs.[31] In the absence of a B2R structure, the high-resolution crystal structure of bovine rhodopsin[23,24] (PDB ID: 1HZX) was used as a template for the B2 receptor model building by using homology modeling techniques. In the first step, a sequence alignment by using the Clustal program[32] was performed. The B2 receptor sequence was taken from the Swiss-Prot Data Base, entry P30411.[4] The most conserved residues in every helix were identified as: 1.50–N75, 2.50–D103, 3.50–R155, 4.50–W182, 5.50–P236, 6.60-P285, 7.50–P329 (the numbers refer to the universal residue labeling scheme proposed by Ballesteros and Weinstein[33] in which the first number refers to the transmembrane helix and the second number relates to the conservation of that residue in this helix). We superposed the B2R sequence with the rhodopsin structure by using the conserved residues as

Table 3. Internal angles of the BK.

	Arg1		Pro2		Pro3		Gly4		Phe5		Ser6		Pro7		Phe8		Arg9	Phe5	EN
	–	ψ	ϕ	ψ	ϕ	ψ	ϕ	ψ	ϕ	ψ	ϕ	ψ	ϕ	ψ	ϕ	ψ	ϕ	χ_1	
NMR	–	88.5	−75.1	−33.4	−75.0	−6.5	−64.3	−15.3	−68.8	150.2	−121.3	165.8	−75.0	−11.7	−75.9	−16.8	49.3 –	–	–
D	–	120.9	−60.2	−46.5	−69.9	−4.5	−74.3	12.1	−48.7	155.0	−126.3	−175.2	−70.7	−30.1	−87.5	−14.6	173.2 –	−58.2	−195.0
L1	–	–	–	–	–	–	–	–	−125.1	114.1	−143.1	169.5	−54.8	68.6	−74.2	−35.2	−154.3 –	–	–
L2	–	144.7	−99.2	157.1	−98.3	155.6	170.3	−147.6	−136.6	−75.7	167.8	141.0	−42.7	−76.9	−65.8	−28.4	−163.7 –	–	−32.5

NMR-SS = NMR structure, D = conformation D, L1, L2 = ref. [72] and [70] respectively. EN = BK internal energy [kcal mol^{-1}] calculated by using the AMBER force field.

markers, to replace amino acid residues in the proper order. An initial 3D homology model was built by using the BIOPOLYMER module from the SYBYL[34] software package including the following modifications: Helix 4 (TM4) was elongated by three residues from the extracellular side and the second extracellular loop (EL2) was moved up by one helix turn to fit the B2R sequence to the rhodopsin structure. It is of interest to note that the new position of EL2 is consistent with the position of the EL2 in the β_2-adrenergic receptor structure (2RH1,[25,26]). Helix 3 (TM3) was rotated clockwise by 30° along its axis (viewed from the extracellular side) to generate the hydrogen bond (with initial distance 2.2 Å) between N(3.35) and W(6.48) as reported in refs. [35–37]. The hydrogen bond between N(3.35) and W(6.48) resembled a key interaction that kept the receptor in its inactive form. Finally, receptor loops and missing fragments were built by using the LOOP SEARCH module from SYBYL.[34] A disulfide bond between C130 (beginning of TM3) and C211 (EL2)[38] and the palmitoyl group (PAL) that is attached to the C351 at the end of H8[39] were added. Due to the high mobility and to decrease the number of water molecules necessary to "cover" the protein, the first 36 and last 33 residues from the N-terminal and C-terminal part of the receptor were deleted, respectively. The N-terminal part is involved in the glycosylation and receptor expression at the cell surface, but it is not required for ligand binding.[40] The C-terminal part of the receptor plays a crucial role in signal transduction. Data that were collected in ref. [41] indicated that this part of the receptor contained three intracellular helices that form the G protein–receptor interface. According to ref. [42] palmitoylation of cysteine residues present at the intracellular side of the protein is important for ligand binding. In the computed model, one palmitoyl group (PAL) and one intracellular helix (H8) were present. The thus-obtained receptor model was energy minimized and refined. To maintain the shape of the core as much as possible during the optimization procedure, positional constraints on all Cα atoms (except extra- and intracellular domain) were applied.

Biochemical and biophysical data indicate that GPCRs can form homodimers and heterodimers.[43] There is evidence that in the cellular membrane, rhodopsin can exist as a dimer, tetramer, or even a hexamer.[44] According to the data presented in refs. [45–47] the bradykinin receptor exists as a homodimer and also as a heterodimer with the angiotensin receptor. However, the receptor dimerization seems not to be required for G protein activation.[48] To decrease the number of atoms in the computed system and due to the lack of sufficient structural characterization of dimeric GPCRs, in our model B2R was considered to be a monomer.

Building a model for the BK–B2R complex ligand docking: The ligand peptide was placed inside the receptor pocket to avoid steric clashes. The receptor pocket is conserved within the class A GPCR family.[49] The diameter of the receptor pocket is approximately 15 and 21 Å in height and width, respectively. These dimensions have to be considered with care because the receptor pocket height depends strongly on the position of the second extracellular loop (EL2). We consider our assumptions to be reasonable however, because further modifications of this region would generate a model that deviates even more from the original rhodopsin structure and that would not be consistent with the position of the EL2 in β_2-adrenergic receptor (β2ADR) structure. The bottom of the receptor binding pocket is highly hydrophobic with hydrophilic residues placed on the three corners (Figure 1).

The hormone has an N-to-C-terminal length of 18 Å and widths of approximately 14 Å if the arginine residues are planar. From the previous NMR spectroscopic data,[28] no information about the side-chain conformation could be derived because the backbone conformation was derived based on TALOS angular restraints;[28] however, even after taking all sterically allowed side-chain conformations into account, only a very limited number of possibilities were found that allowed docking of the ligand into the binding pocket. In particular, a "vertical" placement could be excluded in which the N and C termini of BK are parallel to the membrane normal. In the solid-state NMR experiments, the backbone conformation was derived based on TALOS angular restraints.[28] The side-chain conformations were derived from the force field that was applied during the simulated annealing protocol as implemented in the CYANA program.[50] While the ensemble of structures converged well, the relative side-chain conformations of arginines one and nine did not. Two possible conformations have been found in which both arginine side chains lie within one plane but with either antiparallel ("Z" like) or parallel ("C" like) orientation (Figure 2). Both ligand models could be docked in two different ways each, which resulted in four possibilities (Figure 1 A–D). With a lack of hydrophilic residues at the bottom right of the receptor binding pocket, we assumed that the arginine residue could not be placed in this area. Due to steric interference we were unable to build the conformation that is presented in Figure 1 C. Therefore, the three remaining preassembled ligand–receptor complexes were used for further optimization and energy refinement.

Membrane model: The optimized ligand–receptor complexes were immersed into a fully hydrated ~10 ns equilibrated POPC[51] (1-palmitoyl-2-oleoyl-*sn*-glycero-3-phosphatidylcholine) lipid bilayer. The membrane was adapted to the bradykinin receptor first. Each of the three computed systems consisted of 120 lipid molecules, 330 amino acid residues (321 receptor and 9 bradykinin), 8 Cl^- counter ions (to neutralize positive charge on the receptor) and ~7000 water molecules; this gave ~31 000 atoms total in the periodic rectangular box of approximately 75×65×90 Å.

MD simulations: All simulations were performed by using the AMBER 7.0 force field.[52] The computed systems were optimized by using short (1 ps) and low-temperature (30 K) molecular dynamics (MD) and minimization in cycles. During the optimization procedure, positional constraints were applied to the Cα atoms of the receptor's helical domains. In the next step, a MD simulation for all ligand–receptor–membrane systems was carried out with following conditions: 1 fs time step, constant pressure (1 atm), periodic boundary conditions and the SHAKE algorithm[53] on the hydrogen atoms were applied. For long-range electrostatic interactions, the PME (Particle Mesh Ewald) method was employed.[54] To limit the direct space sum for PME, a 12 Å cutoff was used. Non-bonding interactions were updated every 25 steps. For the protein, hormone, and membrane, united atom[55] force field parameters were used, and for the water molecules, the TIP3P model[56] was used. The total simulation time was 2 ns. During the first 200 ps, the system temperature was linearly increased from 10 to 300 K, then, molecular dynamics at 300 K were computed. During the simulation, all atoms were free to move. An in-house tool was used for the ligand–receptor interaction analysis. If the distance between the closest atoms (except hydrogen) from selected residues was less than 4.1 Å in the analyzed snapshot, then the interaction was identified. In all protein–ligand interface descriptions, the following convention was used: a three-letter abbreviation for a ligand residue, and a one-letter code for a protein residue.

Acknowledgements

The work was supported by the Center for Scientific Computing (CSC) of Frankfurt University, the Academic Computer Center in Gdansk (TASK), the Center for Biomolecular Magnetic Resonance (BMRZ), the DFG Center of Excellence: Macromolecular complexes (CEF-MC) and the European Union Community, Marie Curie Host Fellowships for TOK, contract no. MTKI-CT-2004-509 750.

Keywords: amber force field · bradykinin · GPCR · hormones · molecular modeling · receptors

[1] D. Regoli, J. Barabe, *Pharm. Rev.* **1980**, *32*, 1–46.
[2] K. D. Bhoola, C. D. Figueroa, K. Worthy, *Pharm. Rev.* **1992**, *44*, 1–80.
[3] J. G. Menke, J. A. Borkowski, K. K. Bierilo, T. MacNeil, A. W. Derrick, K. A. Schneck, R. W. Ransom, C. D. Strader, D. L. Linemeyer, J. F. Hess, *J. Biol. Chem.* **1994**, *269*, 21 583–21 586.
[4] J. F. R. Hess, J. A. Borkowski, G. S. Young, C. D. Strader, R. W. Ransom, *Biochem. Biophys. Res. Commun.* **1992**, *184*, 260–268.
[5] "Pharmacology and Immunopharmacology of Kinin Receptors", J. M. Hall, I. K. M. Morton in *The Handbook of Immunopharmacology: The Kinin System* (Ed.: S. G. Farmer), Academic Press, New York, **1997**, pp. 9–43.
[6] F. Philip, P. Sengupta, S. Scarlata, *J. Biol. Chem.* **2007**, *282*, 19203–19216.
[7] J. B. Su, F. Barbe, R. Houel, T. T. Guyene, B. Crozatier, L. Hittinger, *Circulation* **1998**, *98*, 2911–2918.
[8] M. M. Tiwari, P. L. Prather, P. R. Mayeux, *J. Pharmacol. Exp. Ther.* **2005**, *313*, 798–805.
[9] M. R. Kichuk, N. Seyedi, X. Zhang, C. C. Marboe, R. E. Michler, L. J. Addonizio, G. Kaley, A. Nasjletti, T. H. Hintze, *Circulation* **1996**, *94*, 44–51.
[10] L. R. Steranka, D. C. Manning, C. J. DeHaas, J. W. Ferkany, S. A. Borosky, J. R. Connor, R. J. Vavrek, J. M. Stewart, S. H. Snyder, *Proc. Natl. Acad. Sci. USA* **1988**, *85*, 3245–3249.
[11] H. Wang, C. Ehnert, G. J. Brenner, C. J. Woolf, *Biol. Chem.* **2006**, *387*, 11–14.
[12] A. Duka, I. Duka, G. Gao, S. Shenouda, I. Gavras, H. Gavras, *Am. J. Physiol. Endocrinol. Metab.* **2006**, *291*, E268–274.
[13] J. J. Chen, E. J. Johnson, *Expert Opin. Ther. Targets* **2007**, *11*, 21–35.
[14] A. Graness, A. Adomeit, R. Heinze, R. Wetzker, C. Liebmann, *J. Biol. Chem.* **1998**, *273*, 32016–32022.
[15] S. Greco, A. Muscella, M. G. Elia, S. Romano, C. Storelli, S. Marsigliante, *J. Cell. Physiol.* **2004**, *201*, 84–96.
[16] S. Drube, C. Liebmann, *Br. J. Pharmacol.* **2000**, *131*, 1553–1560.
[17] G. A. Argañaraz, S. R. Perosa, E. C. Leocioni, M. Bader, E. A. Cavalheiro, M. da G. Naffah-Mazzacoratti, J. B. Pesquero, J. A. Silva Jr. , *Brain Res.* **2004**, *1013*, 30–39.
[18] S. R. Perosa, G. A. Arganaraz, E. M. Goto, L. G. Costa, A. C. Konno, P. P. Varella, J. F. Santiago, J. B. Pesquero, M. Canzian, D. Amado, E. M. Yacubian, H. Carrete, R. S. Centeno, E. A. Cavalheiro, J. A. Silva, M. G. Mazzacoratti, *Hippocampus* **2007**, *17*, 26–33.
[19] A. Marmarou, M. Guy, L. Murphey, F. Roy, L. Layani, J. P. Combal, C. Marquer, *J. Neurotrauma* **2005**, *12*, 1444–1455.
[20] K. Oguro, H. Hashimoto, M. Nakashima, *Arch. Int. Pharmacodyn. Ther.* **1982**, *256*, 108–122.
[21] S. Filipek, D. C. Teller, K. Palczewski, R. Stenkamp, *Annu. Rev. Biophys. Biomol. Struct.* **2003**, *32*, 375–397.
[22] J. Ballesteros, K. Palczewski, *Curr. Opin. Drug Discovery Dev.* **2001**, *4*, 561–574.
[23] K. Palczewski, T. Kumasaka, T. Hori, C. A. Behnke, H. Motoshima, B. A. Fox, I. Le Trong, D. C. Teller, T. Okada, R. E. Stenkamp, M. Yamamoto, M. Miyano, *Science* **2000**, *289*, 739–745.
[24] D. C. Teller, T. Okada, C. A. Behnke, K. Palczewski, R. E. Stenkamp, *Biochemistry* **2001**, *40*, 7761–7772.
[25] V. Cherezov, D. M. Rosenbaum, M. A. Hanson, S. G. F. Rasmussen, F. S. Thian, T. S. Kobilka, H. J. Choi, P. Kuhn, W. I. Weis, B. K. Kobilka, R. C. Stevens, *Science* **2007**, *318*, 1258–1265.
[26] D. M. Rosenbaum, V. Cherezov, M. A. Hanson, S. G. F. Rasmussen, F. S. Thian, T. S. Kobilka, H. J. Choi, Z. J. Yao, W. I. Weis, R. C. Stevens, B. K. Kobilka, *Science* **2007**, *318*, 1266–1273.
[27] D. Salom, D. T. Lodowski, R. E. Stenkamp, I. L. Trong, M. Golczak, B. Jastrzebska, T. Harris, J. A. Ballesteros, K. Palczewski, *Proc. Natl. Acad. Sci. USA* **2006**, *103*, 16123–16128.
[28] J. J. Lopez, A. K. Shukla, C. Reinhart, H. Schwalbe, H. Michael, C. Glaubitz, *Angew. Chem.* **2008**, *120*, 1548; *Angew. Chem. Int. Ed.* **2008**, *47*, 1668–1671
[29] S. Luca, J. F. White, A. K. Sohal, D. V. Filipov, J. H. van Boom, R. Grisshammer, M. Baldus, *Proc. Natl. Acad. Sci. USA* **2003**, *100*, 10706–10711.
[30] S. N. Ha, P. J. Hey, R. W. Ransom, M. G. Bock, D. S. Su, K. L. Murphy, R. Chang, T. B. Chen, D. Pettibone, J. F. Hess, *Biochemistry* **2006**, *45*, 14355–14361.
[31] U. Gether, *Endocr. Rev.* **2000**, *21*, 90–113.
[32] J. D. Thompson, T. J. Gibson, F. Plewniak, F. Jeanmougin, D. G. Higgins, *Nucleic. Acids Res.* **1997**, *25*, 4876–4882.
[33] J. A. Ballesteros, H. Weinstein, *Methods Neurosci.* **1995**, *25*, 366–428.
[34] SYBYL 6.8 2002, Tripos Inc., 1699 South Hanley Road., St. Louis, MO 63144 (USA).
[35] J. Marie, E. Richard, D. Pruneau, J. L. Paquet, C. Siatka, R. Larguier, C. Poncé, P. Vassault, T. Groblewski, B. Maigret, J. C. Bonnafous, *J. Biol. Chem.* **2001**, *276*, 41100–41111.
[36] L. M. F. Leeb-Lundberg, D. S. Kang, M. E. Lamb, D. B. Fathy, *J. Biol. Chem.* **2001**, *276*, 8785–8792.
[37] S. Meini, P. Cucchi, F. Bellucci, C. Catalani, A. Faiella, L. Rotondaro, L. Quartara, A. Giolitti, C. A. Maggi, *Biochem. Pharmacol.* **2004**, *67*, 601–609.
[38] M. C. S. Herzig, N. R. Nash, M. Connolly, D. J. Kyle, L. M. F. Leeb-Lundberg, *J. Biol. Chem.* **1996**, *271*, 29 746–29 751.
[39] A. Faussner, A. Bauer, I. Kalatskaya, S. Schussler, C. Seidl, D. Proud, M. Jochum, *FEBS J.* **2005**, *272*, 129–140.
[40] S. Michineau, L. Muller, A. Pizard, F. Alhenc-Gelas, R. M. Rajerison, *Biol. Chem.* **2004**, *385*, 49–57.
[41] A. Piserchio, V. Zelesky, J. Yu, L. Taylor, P. Polgar, D. F. Mierke, *Biopolymers* **2005**, *80*, 367–373.
[42] A. Pizard, A. Blaukat, S. Michineau, I. Dikic, W. Muller-Esterl, F. Alhenc-Gelas, R. M. Rajerison, *Biochemistry* **2001**, *40*, 15743–15751.
[43] S. Terrillon, M. Bouvier, *EMBO Rep.* **2004**, *5*, 30–34.
[44] Y. Liang, D. Fotiadis, S. Filipek, D. A. Saperstein, K. Palczewski, A. Engel, *J. Biol. Chem.* **2003**, *278*, 21655–21662.
[45] A. Blaukat, *Andrologia* **2003**, *35*, 17–23.
[46] S. Michineau, F. Alhenc-Gelas, R. M. Rajerison, *Biochemistry* **2006**, *45*, 2699–2707.
[47] P. M. Abadir, A. Periasamy, R. M. Carey, H. M. Siragy, *Hypertension* **2006**, *48*, 316–322.
[48] M. R. Whorton, M. P. Bokoch, S. G. F. Rasmussen, B. Huang, R. N. Zare, B. Kobilka, R. K. Sunahara, *Proc. Natl. Acad. Sci. USA* **2007**, *104*, 7682–7687.
[49] R. P. Bywater, *J. Mol. Recognit.* **2005**, *18*, 60–72.
[50] P. Güntert, *Prog. NMR Spectrosc.* **2003**, *43*, 105–125.
[51] K. Murzyn, T. Róg, G. Jezierski, Y. Takaoka, M. Pasenkiewicz-Gierula, *Biophys. J.* **2001**, *81*, 170–183.
[52] D. A. Pearlman, D. A. Case, J. W. Caldwell, W. S. Ross, T. E. Cheatham III, S. DeBolt, D. Ferguson, G. Seibel, P. Kollman, *Comput. Phys. Commun.* **1995**, *91*, 1–41.
[53] J. P. Ryckaert, G. Ciccotti, H. J. C. Berendsen, *J. Comp. Physiol.* **1977**, *23*, 327–341.
[54] U. Essmann, L. Perera, M. L. Berkowitz, T. Darden, H. Lee, L. G. Pedersen, *J. Chem. Phys.* **1995**, *103*, 8577–8593.
[55] S. J. Weiner, P. A. Kollmann, D. A. Case, U. C. Singh, C. Ghio, G. Alagona, S. J. Profeta, P. Weiner, *J. Am. Chem. Soc.* **1984**, *106*, 765–784.
[56] W. L. Jorgensen, J. Chandrasekhar, J. D. Madura, R. W. Impey, M. L. Klein, *J. Chem. Phys.* **1983**, *79*, 926–935.
[57] D. B. Fathy, S. A. Mathis, T. Leeb, L. M. Leeb-Lundberg, *J. Biol. Chem.* **1998**, *273*, 12210–12218.
[58] G. V. Nikiforovich, G. R. Marshall, *Biochemistry* **2003**, *42*, 9110–9120.
[59] G. Schertler, *Curr. Opin. Struct. Biol.* **2005**, *15*, 408–415.
[60] A. K. Kusnetzow, C. Altenbach, W. L. Hubbell, *Biochemistry* **2006**, *45*, 5538 5550.
[61] K. Werner, I. Lehner, H. K. Dhiman, C. Richter, C. Glaubitz, H. Schwalbe, J. Klein-Seetharaman, H. G. Khorana, *J. Biomol. NMR* **2007**, *37*, 303–312; K.

Werner, C. Richter, J. Klein-Seetharaman, H. Schwalbe, *J. Biomol. NMR* **2008**, *40*, 49–53; J. Klein-Seetharaman, N. V. K. Yanamala, F. Javeed, P. J. Reeves, E. V. Getmanova, M. C. Loewen, H. Schwalbe, H. G. Khorana, *Proc. Natl. Acad. Sci. USA* **2004**, *101*, 3409–3413; J. Klein-Seetharaman, P. J. Reeves, M. C. Loewen, E. V. Getmanova, J. Chung, H. Schwalbe, P. E. Wright, H. G. Khorana, *Proc. Natl. Acad. Sci. USA* **2002**, *99*, 3452–3457; M. C. Loewen, J. Klein-Seetharaman, E. V. Getmanova, P. J. Reeves, H. Schwalbe, H. G. Khorana, *Proc. Natl. Acad. Sci. USA* **2001**, *98*, 4888–4892.

[62] P. S. H. Park, D. T. Lodowski, K. Palczewski, *Annu. Rev. Pharmacol. Toxicol.* **2008**, *48*, 107–141.

[63] P. R. Gouldson, N. J. Kidley, R. P. Bywater, G. Psaroudakis, H. D. Brooks, C. Diaz, D. Shire, C. A. Reynolds, *Proteins Struct. Funct. Bioinf.* **2004**, *56*, 67–84.

[64] A. B. Patel, E. Crocker, P. J. Reeves, E. V. Getmanova, M. Eilers, H. Gobind Khorana, S. O. Smith, *J. Mol. Biol.* **2005**, *347*, 803–812.

[65] H. Wei, S. Ahn, S. K. Shenoy, S. S. Karnik, L. Hunyady, L. M. Luttrell, R. J. Lefkowitz, *Proc. Natl. Acad. Sci. USA* **2003**, *100*, 10782–10787.

[66] Y. H. Feng, Y. Ding, S. Ren, L. Zhou, C. Xu, S. S. Karnik, *Hypertension* **2005**, *46*, 419–425.

[67] I. Kalatskaya, S. Schussler, A. Blaukat, W. Muller-Esterl, M. Jochum, D. Proud, A. Faussner, *J. Biol. Chem.* **2004**, *279*, 31268–31276.

[68] J. M. Kim, C. Altenbach, M. Kono, D. D. Oprian, W. L. Hubbell, H. G. Khorana, *Proc. Natl. Acad. Sci. USA* **2004**, *101*, 12508–12513.

[69] L. Shi, G. Liapakis, R. Xu, F. Guarnieri, J. A. Ballesteros, J. A. Javitch, *J. Biol. Chem.* **2002**, *277*, 40989–40996.

[70] D. J. Kyle, S. Chakravarty, J. A. Sinsko, T. M. Stormann, *J. Med. Chem.* **1994**, *37*, 1347–1354.

[71] H. Ottleben, M. Haasemann, R. Ramachandran, M. Gorlach, W. Muller-Esterl, L. R. Brown, *Eur. J. Biochem.* **1997**, *244*, 471–478.

[72] C. Chatterjee, C. Mukhopadhay, *Biopolymers* **2005**, *78*, 197–205.

[73] J. M. Baldwin, *EMBO J.* **1993**, *12*, 1693–1703.

[74] D. Regoli, S. N. Allogho, A. Rizzi, F. Gobeil Jr. , *Eur. J. Pharmacol.* **1998**, *348*, 1–10.

[75] H. Heitsch, *Curr. Med. Chem.* **2002**, *9*, 913–928.

Received: May 10, 2008
Published online on September 18, 2008

